



Precipitation type detection Present Weather Sensor

Final report

H. Bloemink

Koninklijk Nederlands Meteorologisch Instituut

Technical Report = Technisch Rapport; TR-259

De Bilt, 2004

PO Box 201, 3730 AE De Bilt
The Netherlands
Wilhelminalaan 10
<http://www.knmi.nl>
Telephone +31 30 22 06 911
Telefax +31 30 22 10 407

Author: H. Bloemink

UDC: 551.508.77
551.508.824

ISSN: 0169-1708

ISBN: 90-369-2246-1



Precipitation type detection Present Weather Sensor



Project no. 12809

Final report February 2004

H. Bloemink

MI/INSA/IO

Contents

1	<i>Introduction.....</i>	3
2	<i>Present weather determination.....</i>	3
3	<i>Experiment</i>	4
3.1	Instrument	4
3.2	Available data	6
3.3	Data handling.....	7
3.4	Meteorological conditions	7
3.5	Comparing the Observer and PWC.....	9
4	<i>Particle size distributions</i>	11
4.1	Data.....	11
4.2	Characterization of the distributions.....	11
4.2.1	<i>Fitting the particle size distribution</i>	11
4.2.2	<i>Counting large particles.....</i>	11
4.3	Relation to precipitation type	12
4.4	Combining the various data.....	13
4.4.1	<i>Distribution & PWC</i>	13
4.4.2	<i>Distribution and precipitation amount.....</i>	14
4.4.3	<i>Distribution and opt/drd ratio</i>	15
4.5	Discussion	16
5	<i>Other instruments</i>	17
6	<i>Summary and recommendations</i>	18
	<i>Appendix A: Weather codes.....</i>	19
	<i>Appendix B: Precipitation types and amounts</i>	19

1 Introduction

Determination of the type of precipitation has long been done by meteorological observers. In the early 1970's, the first automated systems to determine present weather were being developed, and nowadays many Automatic Weather Stations (AWS) are equipped with these so-called Present Weather Sensors (PWS). KNMI has the Vaisala FD 1 2P PWS in use at all its synoptic sites. Only at airports are there human observers reporting present weather.

Generally, the precipitation type determined by the FD 1 2P agrees with human observations¹. There are, however, some areas where the sensor performs not as well. Especially the narrow region around 0 °C (where mixed-phase precipitation can occur) is identified as a problem area. In case of mixed precipitation (rain and snow), the sensor tends to report either rain or snow. In order to investigate this in more detail, Vaisala has provided software to extract (amongst other data) the particle size distribution of the precipitation. These distributions are the basis for the research described in this report. It is investigated whether the particle size distribution, and particularly the shape of the distribution, provides information to improve the present weather determination.

Also, a short investigation into other systems (e.g. other PW systems, hail detector) has been done.

2 Present weather determination

In this section, the determination of the present weather, and in particular the precipitation type, of the Vaisala FD 1 2P is described. This type of sensor measures the scattering of light of a small volume of the atmosphere. If there are precipitation particles present in this volume, they will lead to peaks in the scattered light. These peaks are related to (the size of) the particles. Separately, the FD 1 2P has a capacitive sensor (DRD 1 2) that measures the water content of the precipitation. Combining these two quantities leads to a discrimination between large particles with low water content (i.e. snow) and small particles with high water content (rain). This is shown in Figure 1 (the y-scale).

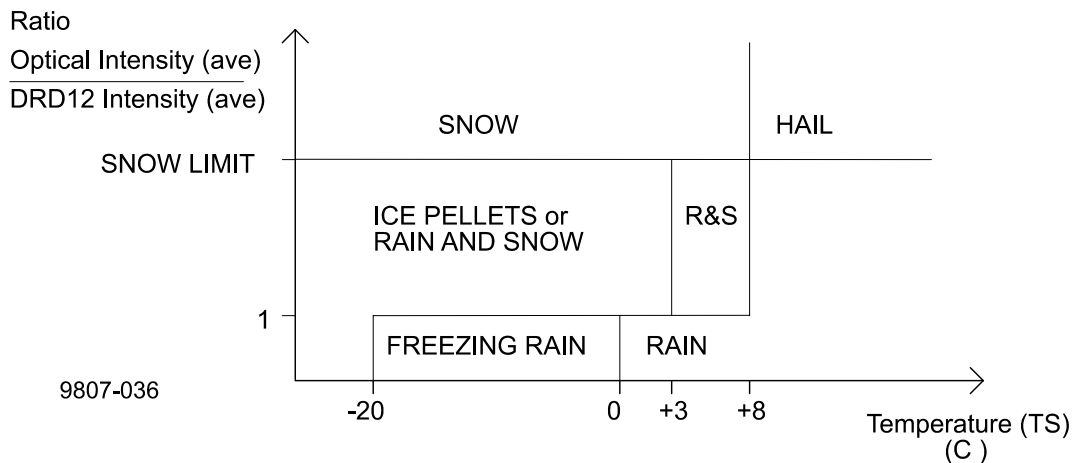


Figure 1. Principal precipitation type determination of the FD 1 2P (from FD 1 2P User's Guide).

¹ See report WMO Intercomparison of Present Weather Sensors/Systems ('PREWIC'; WMO/TP-No. 887, 1998).

Further discrimination of precipitation type involves temperature constraints (the x-scale in Figure 1), maximum particle size and a selection algorithm to determine the most significant precipitation type. More details can, for instance, be found in the FD 1 2P User's Guide².

The above description did not perform too well with regards to freezing rain. Earlier research has shown that replacing the temperature on the x-axis of Figure 1 with the wet-bulb temperature, and choosing appropriate limits, significantly improves the freezing rain detection³. This is shown in Figure 2. The wet bulb temperature is determined using an (external) thermometer and humidity sensor.

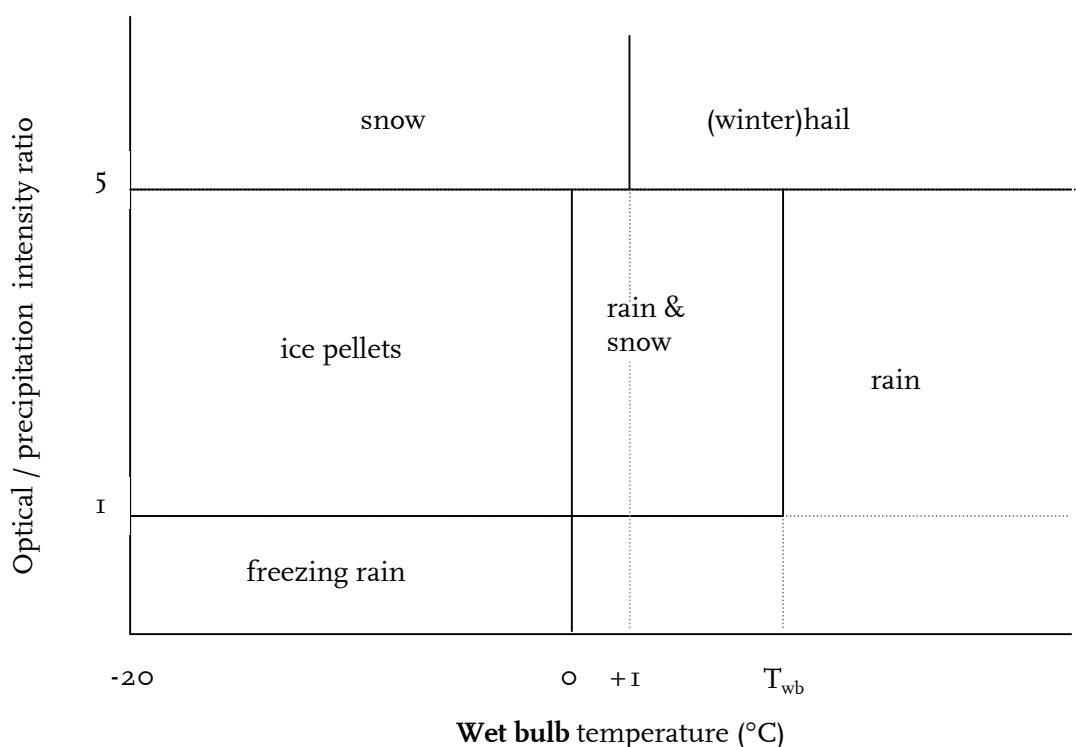


Figure 2. Precipitation type determination of the FD 1 2P currently in use at KNMI. The limit T_{wb} (in °C) depends on the precipitation intensity PI (in mm/h) in the following way: $T_{wb} = 2.7 + 0.4 \cdot \ln(PI + 0.0012)$.

3 Experiment

3.1 Instrument

A Vaisala Fd 1 2P Present Weather Sensor was operated at the test field of KNMI at De Bilt (see Figure 3) as a part of KNMI station no. 261.

² Vaisala, Weather Sensor FD 1 2P, User's Guide, M210296en-A, May 2002.

³ Ruud Ivens, note to Expert group X-AVW, no. AVW20020829, August 2002.

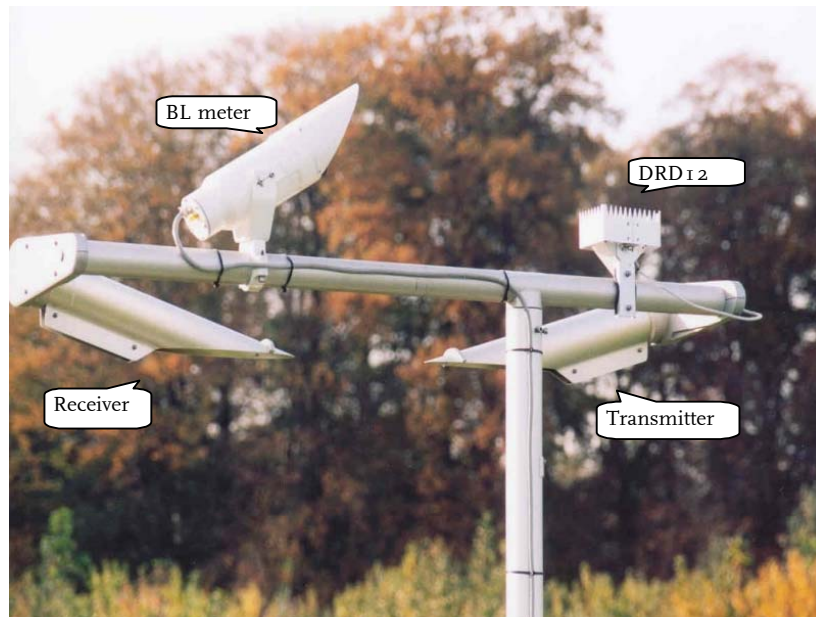


Figure 3. *The FD12P Present Weather sensor.*

This sensor was running software version 1.83S provided by Vaisala for this research. An example of the output is shown in the next table.

09:28:47														time
FD 1_00	1301	1297	S-	71	71	71	0.50	2.03	212	0.4	1954			line 1
-SN														2
12.48	1.070	60	48											3
09:28:59														4
														time
FD 1_00	1280	1297	S-	71	71	71	0.41	2.03	212	0.4	1939			line 1
-SN														2
13.29	1.665	53	54											3
001	433													4
002	120													droplet size distribution
003	199													
004	161													
005	88													
006	85													
007	59													
008	29													
009	28													
010	23													
011	21													
012	22													
013	14													
014	12													
015	15													
016	7													
017	17													
018	11													
019	7													
020	6													
021	1													
022	2													
023	5													
024	9													
025	6													
026	3													
027	5													
028	3													
029	1													
030	2													
031	4													

032	1
034	3
035	2
036	3
037	1
038	5
039	1
040	1
041	1
042	1
043	3
045	2
046	1
049	1
050	2
051	4
052	1
054	1
055	1
057	2
067	1
089	1
0	

Table 1. Example of the FD12P output using the MES8 command of the 1.83S software. These data are from the 3rd February 2001.

Every 12 seconds, a basic message is given, consisting of a PC time stamp and (amongst others) the following information:

1st line: sensor identifier, status bits, visibility (1 minute average), visibility (10 minute average), instant present weather (PW) in NWS code, instant PW in code (0 ... 99), 15 minute PW in code (0 ... 99), 1 hour PW in code (0 ... 99), precipitation water intensity in mm/h (1 minute average), cumulative water sum, cumulative snow sum, cross arm temperature in °C, background luminance in cd/m².

4th line: average optical intensity, average DRD rain detector signal, droplet amount, maximum droplet size (in internal units). All these are data from the previous 15 seconds.

Every 5 minutes, an extended message is given. This message consists of the droplet size distribution of the previous 5 minutes. The 1st number is the droplet size (in internal units), and the 2nd number is the cumulated amount of droplets of that size. The maximum size is 127, and the number of droplets larger than 127 is given at the end of the message.

Internal size units can be converted to SI units using $r = \frac{0.25}{\sqrt{15}} \sqrt{N}$, with r the particle radius in mm and N the size in internal units.

3.2 Available data

Data are used from 3 winters:

- Winter 1: 1 November 2000 – 30 April 2001
- Winter 2: 1 October 2001 – 30 April 2002
- Winter 3: 1 October 2002 – 2 March 2003

The required data is extracted from three different sources:

- Observer. These data is from the files created by the Climatology Department (KD). During winter 3, no observers were present in De Bilt.
- PWC. These data are the data from the Automatic Weather Station. For the PW data this means that the PW output of the FD12P is taken, and corrected. These are the operational

algorithms in use at the KNMI synoptic stations during the time period considered. Since then, the corrections as shown in Figure 2 have been implemented.

- PWS. The data collected using the test software from Vaisala, see section 3.1.

3.3 Data handling

The three different data types (Observer, PWC and PWS) are collected at different times and time intervals. To compare the results, the following calculations were performed:

- Observer: these data were observed between 15 and 5 minutes to the hour. These data (WW) are recorded in the WMO synop codes 4677 and transformed into the codes of Appendix A. These are further used as is.
- PWC. These data are recorded every 12 seconds. They are converted to 10-minute averages. The values from 20 to 10 minutes to the hour are used.
- PWS. The particle size distribution is given every 5 minutes, but not at pre-selected times. Two distributions are used: the one between 15 and 10 minutes to the hour, and the one after that (between 10 and 5 minutes to the hour).

In conclusion: the observations for the hour hh:

- observer: hh-1:45 – hh-1:55 (from KD files)
- PWC data (see tables below): hh-1:50 (from AWS files), 10 minute interval
- PWS data (in particle size distributions): in the 15 minute interval between hh-1:40 – hh:55, 2 5-minute measurements from fd12p_tst

hh-1:40	hh-1:45	hh-1:50	hh-1:55	
				Observer
				PWC
				PWS – particle size distr.

Table 2. Observation periods for comparison with the observer.

Since these time intervals do not completely overlap, they may occasionally cause some differences in present weather extracted from the various data types. Unfortunately, this can not be avoided.

3.4 Meteorological conditions

In the tables and figures below, the type and number of occurrences of precipitation during the three winters in question is shown. A distinction between the PWC data and observer data is made. As mentions earlier, all the PW data are converted to the codes of Appendix A. This means that also the data from the observer is converted. For example, all rain codes (except freezing rain) are converted to code 60. Obviously, the observer does not report code 40 (unknown precipitation). The use of the weather codes is explained in Appendix A. The tables on which the figures are based can be found in Appendix B.

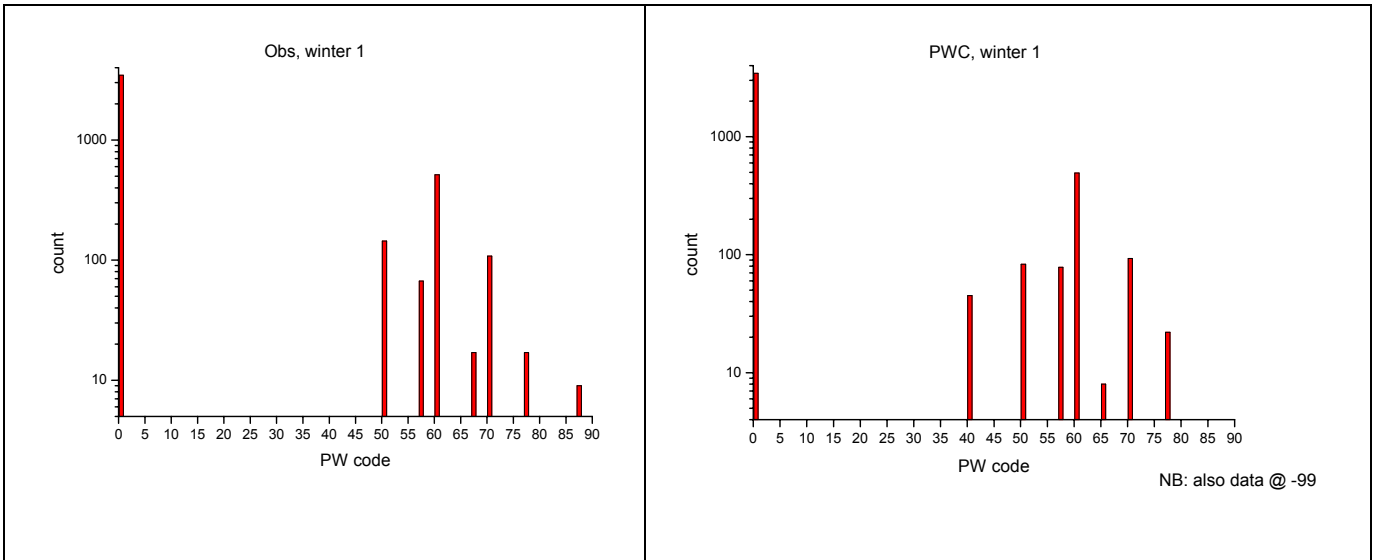


Figure 4. Precipitation distribution during winter 1. The codes on the x-axis are explained in Appendix A. The numbers on the y-axis are based on hourly values.

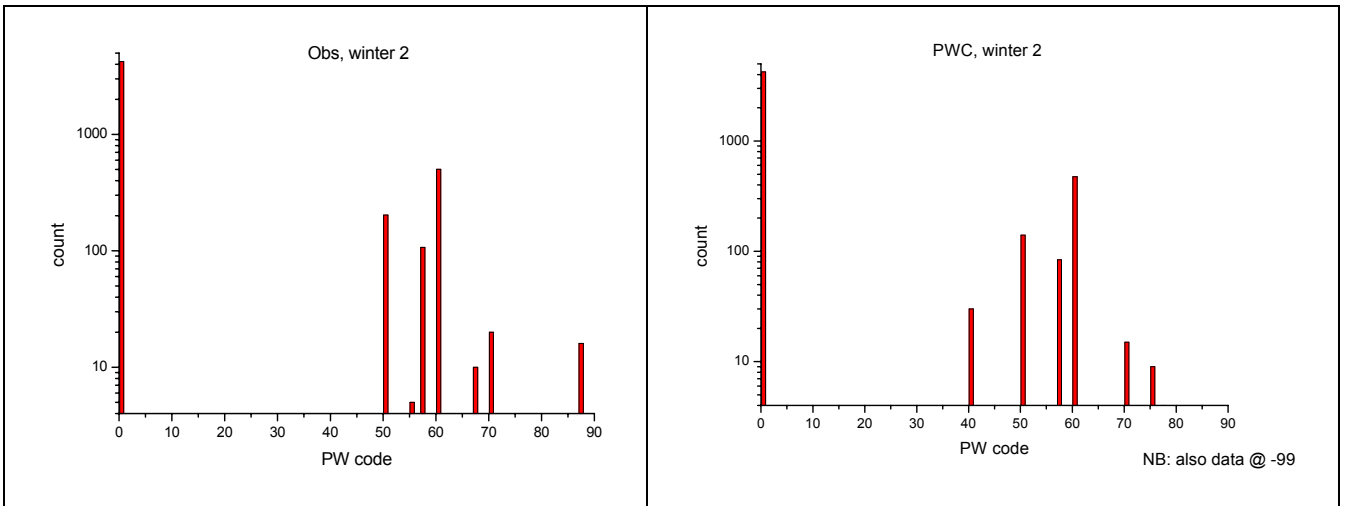


Figure 5. As Figure 4, but for winter 2.

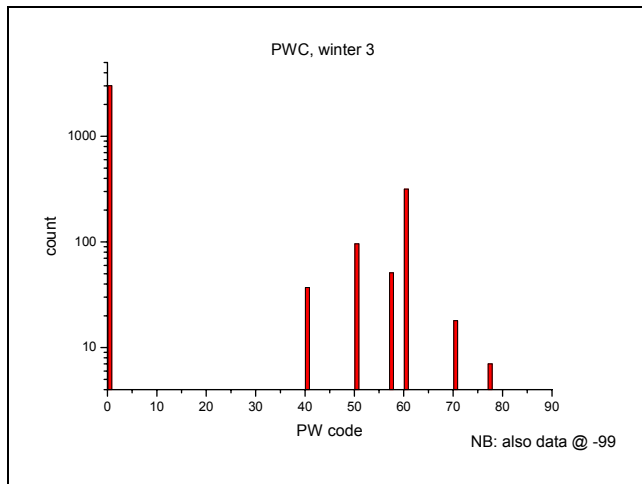


Figure 6. As Figure 4, but for winter 3.

There are a few differences, but generally the Obs data and PWC data show the same picture. Bear in mind that the observer does not report unidentified precipitation (code 40). In winter 1, about 3 % of the time freezing, mixed-phase or solid precipitation (code ≥ 65) was observed. In winter 2, this was about 0.8 % and in winter 3 again 0.8 %. So winter 1 provides the best data set for this study.

3.5 Comparing the Observer and PWC

With the data handling described in section 3.3 (*i.e.* synchronizing the data), it is possible to compare the PWC with the observer for the first two winters. This is shown in the next table.

PWC/Obs	0	40	50	55	57	60	65	67	70	75	77	78	87	89	total
0	7331		181	3	10	120		2	20		6		3		7676
40	24		8	1	7	23		1	5				6		75
50	31		76		36	79			1						223
55															
57	6		17		31	107		1							162
60	127		53	1	81	673	1	8	1	1	1		12	2	961
65						3	3		1	1					8
67															
70	7					2		6	86	1	3		2		107
75	3					3	1	2	2				2		13
77	9		1					2	7		5				24
78	1								3		1				5
87															
89															
total	7539		336	5	165	1010	5	22	126	3	16		25	2	9254

Table 3. Observed precipitation (horizontal) vs. PWC (vertical). The codes are explained in Appendix A. The numbers are based on hourly values.

Extracting the rain and snow cases (code 67) according to the observer leads to the following comparison with the PWC data:

Winter 1:

yy	mo	dd	hr	Obs	PWC	PI	Ta	Tw
00	12	25	04	67	40	1E-3	0,8	0,087
00	12	27	13	67	70	0,03	-0,5	-1,182
01	02	02	15	67	77	0,024	0,1	-0,099
01	02	02	16	67	70	0,659	-0,1	-0,18
01	02	02	18	67	70	0,136	0,1	0,06
01	02	02	19	67	77	0,021	0,1	0,06
01	02	23	13	67	0	0	4,3	2,548
01	03	01	08	67	57	0,19	1,1	1,015
01	03	01	09	67	60	0,443	0,9	0,774
01	03	18	08	67	60	1,288	1,9	1,728
01	03	19	04	67	60	0,94	1,9	1,643
01	03	19	12	67	0	0	4,1	1,787
01	04	14	15	67	-99	-99	-99	-99
01	04	14	16	67	-99	-99	-99	-99
01	04	14	17	67	-99	-99	-99	-99
01	04	14	18	67	-99	-99	-99	-99
01	04	14	20	67	-99	-99	-99	-99

Table 4. All rain and snow cases according to the observer (Obs) compared to the PWC data for winter 1: PW is the weather code according to Appendix A, PI is the precipitation intensity in mm/hr, Ta is the air temperature in °C and Tw is the wet bulb temperature in °C. yy=year, mo = month, dd = day en ht = time in UTC. -99 means: no data available.

Winter2:

yy	mo	dd	hr	Obs	PWC	PI	Ta	Tw
01	11	09	06	67	60	2,292	1,6	1,473
01	12	20	19	67	75	0,341	1,2	0,873
01	12	24	07	67	60	0,028	1,4	0,79
01	12	26	08	67	75	0,617	0,9	0,693
01	12	26	14	67	60	0,007	1,4	1,107
01	12	26	24	67	70	0,035	0,6	0,356
01	12	29	18	67	70	0,246	0,3	0,3
02	02	21	24	67	70	0,044	4,1	-99
02	02	22	01	67	60	1,426	2,3	-99
02	02	22	02	67	60	0,301	2,3	-99

Table 5. Same as Table 4, but now for winter 2.

Unfortunately, the data on April 14th 2001 cannot be used, because the AWS was not working properly. Clearly, for most rain & snow events the PW sensor reports either rain or snow, and occasionally ice pellets, snow grains or no precipitation.

4 Particle size distributions

4.1 Data

In order to make a good comparison with the observer, PWS data from between 15 and 5 minutes to the hour is used (*i.e.* two 5-minute measurements, see section 3.3). Examples of the particle size distributions are shown in Figure 7. As can be expected, snow exhibits more larger particles than rain. Not all distributions show such a clear behaviour, though, which will become apparent in the course of this report.

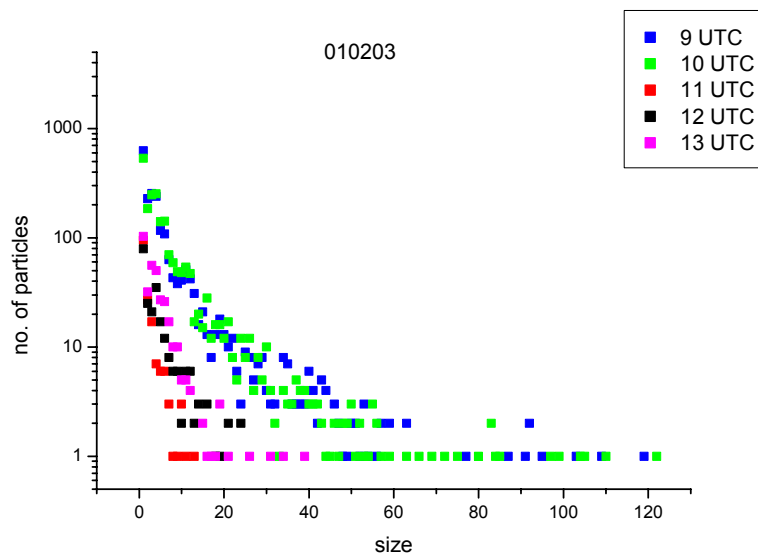


Figure 7. Particle size distributions for the indicated times on the 3rd of February 2001. Y-axis: number of particles, x-axis: particle size in internal units. The observer reported snow at 9 and 10 UTC, snow grains at 11 UTC, ice pellets at 12 UTC and rain at 13 UTC. PWC reported the same except at 12 UTC where it reported rain.

4.2 Characterization of the distributions

Two different characterizations of the particle size distributions were used. One is a fit to the distribution, and the second is counting the number of large particles.

4.2.1 Fitting the particle size distribution

To have a mathematical handle on the particle size distributions, they are fitted to an exponential function: $y = a_1 \cdot e^{-x/T_1}$. Since the y-axis in Figure 7 is a logarithmic scale, the \log of the number of particles is fitted, and the x-axis the size in internal units will be used. Fit parameter T_1 is now a measure of the decay of the distribution. For example, the T_1 values for the distributions in Figure 7 are: 17, 19, 4, 9 and 11 for 9, 10, 11, 12 and 13 UTC, respectively. So indeed the T_1 value is smaller for rain than for snow in this example.

4.2.2 Counting large particles

Another way to characterize the particle size distribution is to count the number of large particles. This is equivalent of integration the particle size distribution over a certain range of particle sizes. Since the number of large particles will also depend on the total amount of particles (*i.e.* the

precipitation intensity), a normalization to the total integral is made. The range chosen for the integral is from 20 – 60 in internal units. In the example of Figure 7, the rain cases would lead to an integration ratio of about 0, whereas the snow cases would lead to a larger number. When particles are larger than about 60, their numbers are very small (1 or 2) and it is more of a coincidence that they occur than statistically significant. This is why the range for the integral is limited to 60.

The integration ratios for the distributions in Figure 7 are: 0.11, 0.11, 0.00, 0.03 and 0.02 for 9, 10, 11, 12 and 13 UTC, respectively.

4.3 Relation to precipitation type

Next, these characterizations need to be matched with the precipitation type. To do so, the relevant parameters (for the fits T_1 , for the large particles the integration ratio) are compared to the precipitation type according to the observer. The results are shown in Figure 8 and Figure 9.

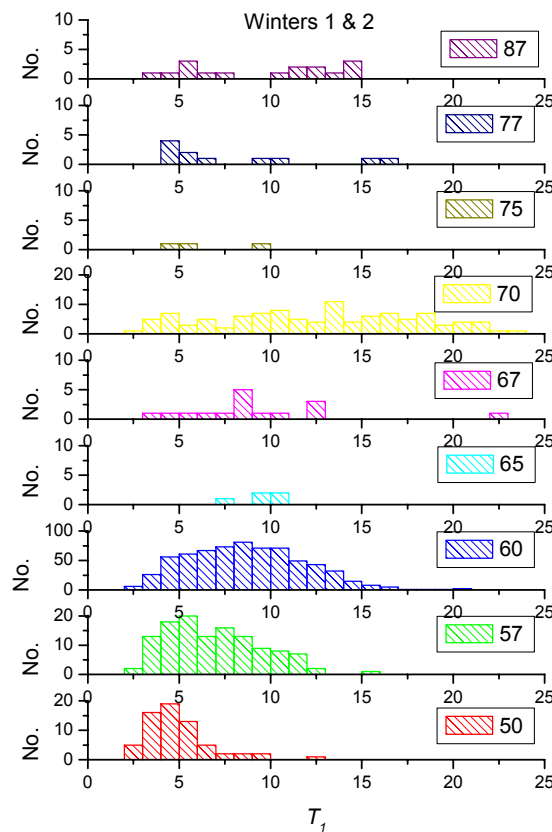


Figure 8. Number of particles (y-axis) as a function of fit parameter T_1 (x-axis) for the indicated precipitation type according to the observer. Note the different scales on the y-axes.

In Figure 8, one can see that in case of rain (codes 50, 57, 60 and 65) there are predominantly smaller particles. Drizzle (code 50) has the smallest particles, followed by a mixture of drizzle and rain (code 57) and then rain (code 60). Snow (code 70) has a much broader distribution with both smaller and larger particles. Mixtures of rain and snow (code 67) appear to have on average somewhat smaller T_1 values, with one exception (of about 22). This is not surprising, since these mixtures can consist of a lot of snow with a little rain but also of a lot of rain with a little snow.

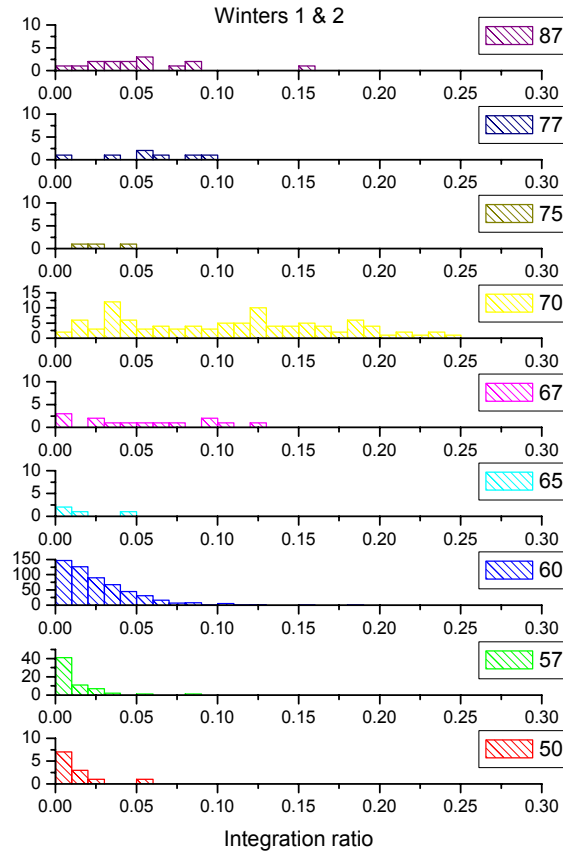


Figure 9. Number of particles (y-axis) as a function of the integration ratio described in the text (x-axis) for the indicated precipitation type according to the observer. Note the different scales on the y-axes

Figure 9 shows a clearer distinction between snow and rain than Figure 8. Rain (codes 50 – 65) has a small integration ratio and snow (code 70) has a large range of values.

4.4 Combining the various data

It is clear from Figure 8 and Figure 9 that using only the particle size distribution will not result in a good precipitation type determination. So these data needs to be combined with other available data. Since the integration ratio shown in Figure 9 shows a better distinction between precipitation type than the Fit parameter T_1 (Figure 8), the integration ratio will be used for this.

4.4.1 Distribution & PWC

A possible means for improvement of the precipitation type detection is combining the precipitation type PWC with the particle size distribution. If, for example, the PWC reports rain, but the integration ratio of the particle size distribution is large, then a correction to rain and snow could be given. This will only work, however, if such an algorithm does not falsely correct good detections.

Since rain and snow (code 67) is of particular interest, the following corrections were tried out.

1. If PWC=70 and integration ratio < 0.03 correct to 67
2. If PWC=50 – 65, and integration ratio > 0.08, correct to 67

The results for winter 1 are shown in the following table (there was very little wintry precipitation in winter 2).

PWC	Integration ratio	no. cases	Observer
60	> 0.08	12	9 × 60 1 × 89 2 × 0
70	< 0.03	9	7 × 70 1 × 67 1 × 0

Table 6. Combining PWC and particle size distribution: rain and snow.

Clearly, this does not work. Far too many right identifications would be falsely corrected. The additional information about the shape of the particle size distribution does not add to the determination of the precipitation type in case of rain and snow (code 67).

Another possibility to improve precipitation type detection is a similar correction, but then for rain and drizzle. Figure 9 shows that drizzle (code 50) and rain and drizzle (code 57) generally have smaller integration ratios than rain. So the following corrections were tried out:

1. If PWC = 50, and integration ratio > 0.004, then correct to 60
2. If PWC = 57, and integration ratio > 0.004, then correct to 60

The results for winters 1 and 2 are shown in the next table.

PWC	Integration ratio	no. cases	Observer
50	> 0.004	4	3 × 60 1 × 70
57	> 0.004	32	2 × 57 29 × 60 1 × 0

Table 7. Combining PWC and particle size distribution: rain.

This correction clearly improves the PW detection. There are very few (4) cases with PWC 50, so it is hard to draw any conclusions from it. However, 90 % of the cases of rain and drizzle are rightly corrected to rain.

4.4.2 Distribution and precipitation amount

The amount of precipitation influences the shape of the particle size distribution. Theoretical relations exist for the different precipitation types⁴, but deviations from these relations are also very common. Furthermore, since these relations differ for the different precipitation type, it is not beforehand obvious which one has to be used. But even if the theoretical relations cannot be used, combining precipitation amount and the shape of the particle size distribution may yield information about the precipitation type. Two parameters are available regarding the precipitation amount: the DRD 12 data (see sections 2 and 3.1) and the precipitation intensity from the AWS. The results are shown in the next figure.

⁴ Marshall, J.S., and W.M. Palmer, *J. Meteor.* 5, 165 (1948); Gunn, J.L.S., and J.S. Marshall, *J. Meteor.* 15, 452 (1958).

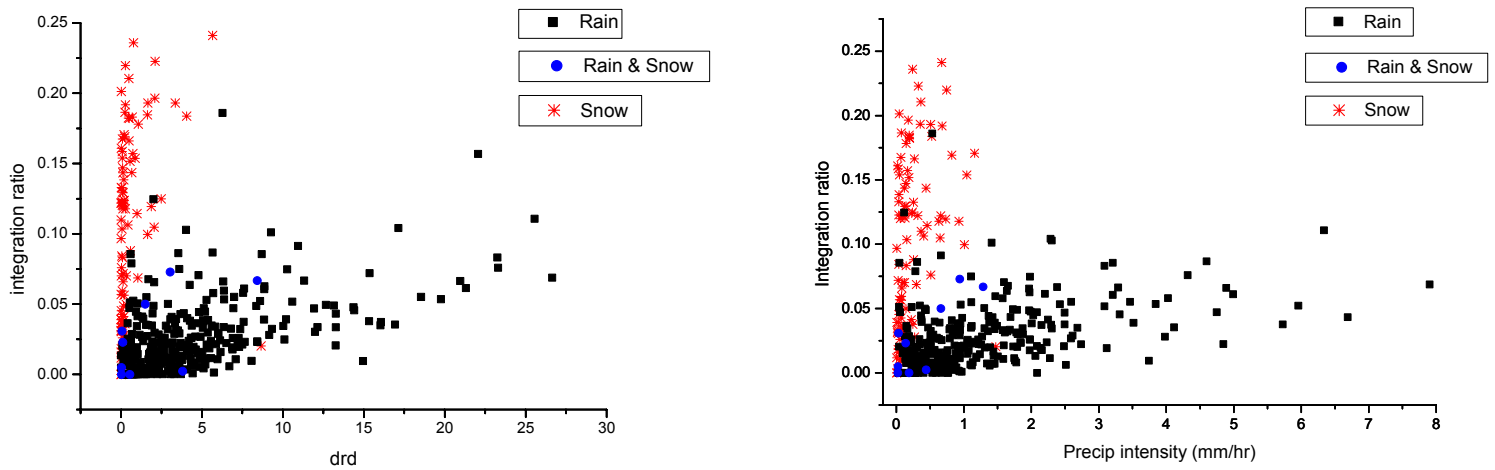


Figure 10. Integration ratio vs. *drd* (left) and precipitation intensity (right). The colour code indicates the observed precipitation type.

As expected, the two figures look very similar. A clear distinction between rain and snow is visible, especially in the figure on the left where the data are exactly synchronized (see section 3.3). This might make it possible to use the integration ratio and *drd* for precipitation type identification. However, the rain and snow identifications (●), which are our main concern in this research, coincide for a large part with the identifications of rain. So, even if the combination of the shape of the particle size distribution with precipitation amount gives better distinction between rain and snow, it does not add to the identification of the Rain and Snow identification.

4.4.3 Distribution and *opt/drd* ratio

In the operational software from Vaisala, the ratio of the optical intensity to the *drd* intensity is used for the main distinction between the precipitation types (see Figure 1 and Figure 2). So it makes sense to combine this quantity with the information regarding the shape of the particle size distribution. This is shown in Figure 11.

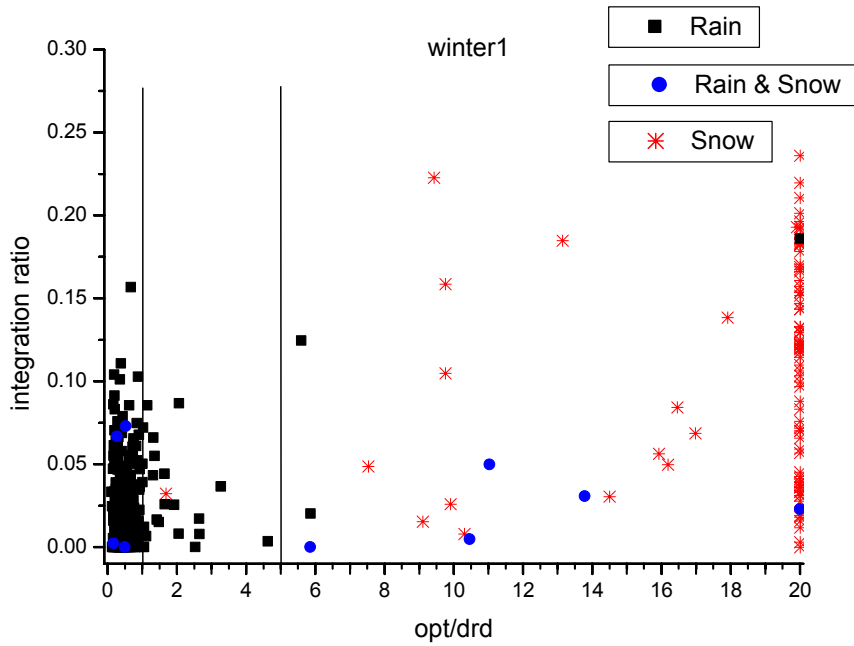


Figure 11. Integration ratio (y-axis) v.s. opt/drd ratio (x-axis) for all observed precipitation types indicated during winter 1. The vertical lines are the limits used by Vaisala (see e.g. Figure 1).

It is clear from this figure why the Rain and Snow identification does not work in the FD12P. All these identifications have either a opt/drd ratio smaller than 1 (which is interpreted as rain) or larger than 5 (interpreted as snow). The additional information on the shape of the particle size distribution also does not produce better results, since the integration ratio for the Rain and Snow cases does not correlate with the opt/drd ratio.

4.5 Discussion

Including the shape of the particle size distribution does not improve the precipitation type identification of the FD12P Present Weather Sensor in the case of Rain and Snow detection. It appears that all the particle size information collected by the instrument is already being used in the identification process.

It is unrealistic to expect a perfect result with respect to the identification of mixtures of Rain and Snow with the current set-up. For example, if an observer sees 2 snowflakes in heavy rain, he will report Rain and Snow, but the FD12P does not have the capability to observe individual particles and so few particles will be averaged out in the instrument. Also, the FD12P has a much smaller sample volume than the observer which is particularly evident in such cases.

As a by-product, a possibility to improve the Rain detection (instead of Rain and Drizzle) was found using the particle size distribution. However, this distinction is not very important for our users.

5 Other instruments

Part of this investigation was the search for (commercially available) instruments to complement, or even replace the ones currently in use.

In particular, a hail detector from Optical Scientific, Inc (OSI) looked promising, since the FD 1 2P does not detect hail very well. The detector's principle is based on acoustics, and it was developed to expand the capabilities of the LEDWI PWS in use in the United States ASOS weather stations. However, a test done over 2 winters by the National Weather Service led to the conclusion that the sensor "showed no significant improvement" over the LEDWI sensor. Therefore the acoustic sensor is no longer being considered as an upgrade to the ASOS stations.⁵ Also, we learned after contacting OSI that the sensor cannot be purchased separately from the LEDWI system.

In the area of PWS research and development, an extensive study in the framework of the European EUMETNET project has recently been concluded. The final report, *Present Weather – Science ; Exploratory actions on automatic present weather observations*⁶, concludes that there are few new developments in the field, other than fine tuning of existing systems. Systems better than the ones currently in use were not found, and are not expected in the near future. The German weather service (DWD) is currently conducting a fairly large-scale intercomparison of different Present Weather Systems, and is interested in cooperating with KNMI.

⁵ Charles G. Wade, *Detecting Ice Pellets, Snow and Hail on ASOS using an Acoustic Sensor*, AMS annual conference, 13 February 2003, Long Beach, US.

⁶ J.P. van der Meulen, final report of EUMETNET project E-PWS-SCI, May 2003, available from www.eumetnet.eu.org/.

6 Summary and recommendations

Measurements from three winters (2000-2001, 2001-2003 and 2002-2003) have been collected and sorted by precipitation type. In winter 1, there was wintry precipitation about 3 % of the time, in winter 2 this was about 0.8 %, the same as in winter 3. In total, there were 27 cases the observer reported a mixture of rain and snow. In none of these cases did the Present Weather Sensor report rain and snow.

Particle size distributions of all precipitations events in these three winters were collected and characterized. This was subsequently linked to the observed precipitation type. Differences between the various types were observed, but they were not unique.

Next, this information was combined with other data (*e.g.* precipitation amount, optical information). This resulted in a clearer distinction between rain and snow, but mixtures of rain and snow did not show any unique behaviour that could be used to distinguish this particular precipitation type. It was concluded that for this precipitation type, all the information collected by the instrument in the current set-up is already being used. An improvement the detection of rain, rather than rain and drizzle mixtures, is possible.

Other instruments that might complement or replace the FD12P were also considered. A promising hail detector was found to have been rejected by the National Weather Service, and in the area of PWS research there are few new developments. Systems better than the ones currently in use were not found, and are not expected in the near future.

Recommendations and future work:

- Research aimed at improving PW output of the FD12P should focus on combining data from different instruments, as no new information can be obtained from the FD12P itself.
- Therefore, new developments in additional systems should be closely monitored, both in R&D and on the commercial market.
- The same holds true for Present Weather systems.
- A closer collaboration with the R&D divisions of other national meteorological services in the field of Present Weather (in particular the DWD and UK Met Office, who are doing similar research) is strongly recommended. A collaboration with the DWD has already been started.

Appendix A: Weather codes

All the weather codes in this report are used according to the table below.

PW code	NWS code	Precipitation type
00	'C'	no precipitation
40	'P'	precipitation
50	'L'	drizzle
55	'ZL'	freezing drizzle
57	'RD'	drizzle and rain
60	'R'	rain
65	'ZR'	freezing rain
67	'RS'	rain and snow
70	'S'	snow
75	'IP'	ice pellets
77	'SG'	snow grains
78	'IC'	ice crystals
87	'SP'	snow pellets
89	'A'	hail

Appendix B: Precipitation types and amounts

Precipitation during winter 1

code	number obs	number PWC	% obs	% PWC
00, 'C'	3457	3442	79.6	80.6
40, 'P'	0	45	0	1.1
50, 'L'	144	83	3.3	1.9
55, 'ZL'	0	0	0	0
57, 'RD'	67	78	1.5	1.8
60, 'R'	514	494	11.8	11.5
65, 'ZR'	5	8	0.1	0.2
67, 'RS'	17	0	0.4	0
70, 'S'	108	93	2.5	2.2
75, 'IP'	3	4	0.1	0.1
77, 'SG'	19	22	0.4	0.5
78, 'IC'	0	0	0	0
87, 'SP'	9	0	0.1	0
89, 'A'	0	0	0	0
total	4343	4269	99.8	99.9

Table 8. Precipitation distribution in winter 1. The codes in column 1 are explained in Appendix A. The number in columns 2 and 3 are based on hourly values. Columns 3 and 4 are the percentages of the total.

Precipitation during winter 2

code	number obs	number PWC	% obs	% PWC
00, 'C'	4223	4234	83.0	84.8
40, 'P'	0	30	0	0.6
50, 'L'	203	140	4.0	2.8

55, 'ZL'	5	0	0.1	0
57, 'RD'	107	84	2.1	1.7
60, 'R'	501	475	9.9	9.5
65, 'ZR'	0	0	0	0
67, 'RS'	10	0	0.2	0
70, 'S'	20	15	0.4	0.3
75, 'IP'	0	9	0	0.2
77, 'SG'	1	3	0.0	0.1
78, 'IC'	0	0	0	0
87, 'SP'	16	0	0.3	0
89, 'A'	0	0	0	0
total	5086	4990	100	100

Table 9. As Table 8, but for winter 2.

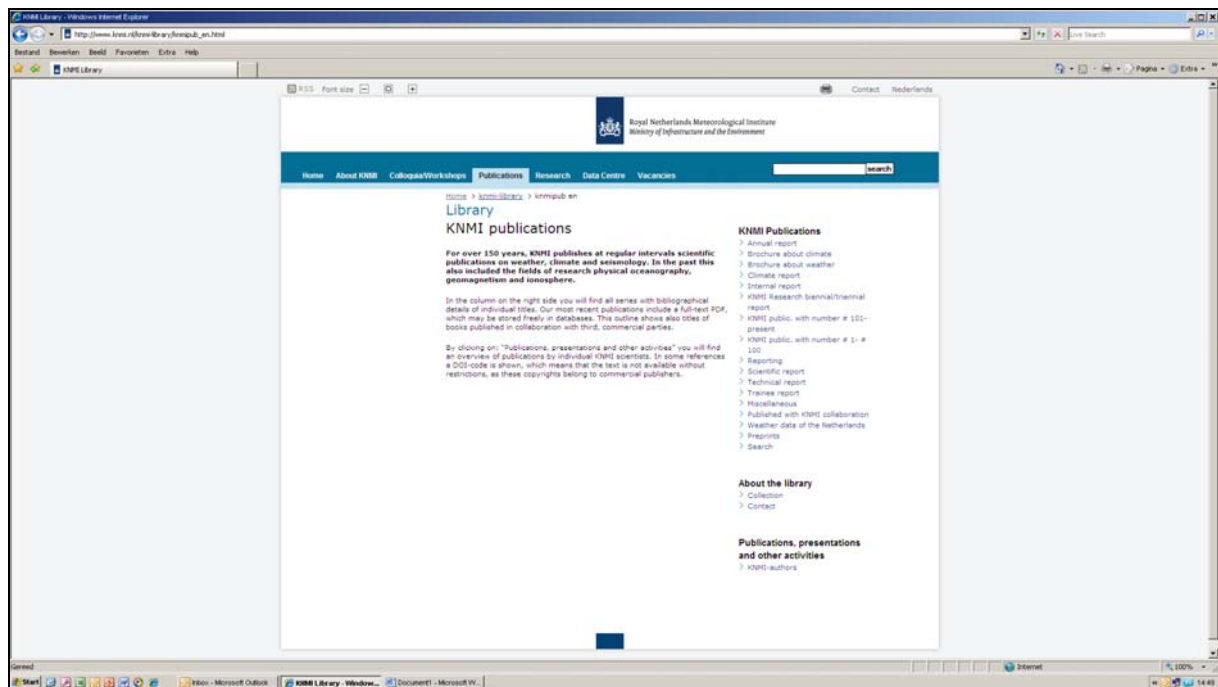
Precipitation during winter 3

code	number PWC	% PWC
00, 'C'	3013	85.1
40, 'P'	37	1.0
50, 'L'	96	2.7
55, 'ZL'	1	0.0
57, 'RD'	51	1.4
60, 'R'	317	9.0
65, 'ZR'	0	0
67, 'RS'	0	0
70, 'S'	18	0.5
75, 'IP'	1	0.0
77, 'SG'	7	0.2
78, 'IC'	0	0
87, 'SP'	0	0
89, 'A'	0	0
totaal	3541	99.9

Table 10. As Table 8, but for winter 3.

A complete list of all KNMI -publications (1854 – present) can be found on our website

www.knmi.nl/knmi-library/knmipub_en.html



The most recent reports are available as a PDF on this site.

